Der-Cherng Liaw
Yew-Wen Liang
Chiz-Chung Cheng

Department of Electrical
and Control Engineering,
National Chiao Tung University,
Hsinchu 30010, Taiwan, Republic of China

Nonlinear Control for Missile Terminal Guidance

Variable Structure Control (VSC) technique is applied to the design of robust homing missile guidance laws. In the design procedure, the target's maneuver is assumed to be unpredictable and is considered as disturbances. Guidance laws are then proposed to achieve the interception performance for both cases of longitude-axis control being available and unavailable. The proposed guidance laws are continuous which alleviate chattering drawback by classic VSC design. Results are obtained and compared with those by realistic true proportional navigation design to illustrate the benefits of the proposed design. [S0022-0434(00)00604-3]

1 Introduction

In recent years, the study of the design of guidance law for interception has attracted much attention. Proportional navigation (PN) has been widely used as the guidance scheme in the homing phase of flight for most missile systems because of its simplicity and easy implementation. These include quasi-optimal PN (Axelband and Hardy [1]), augmenting PN (Arbenz [2]), predicted PN (Kim et al. [3]), general PN (Yang and Yeh [4]), pure PN (Becker [5]), ideal PN (Yuan and Chern [6]), and true PN (Yuan and Chern [7]). Among them, two generic classes of PN laws exist depending on whether the control acceleration of the pursuer is referenced relative to the pursuer velocity vector (e.g., pure PN and ideal PN) or the target-pursuer line-of-sight (e.g., general PN and true PN). Moreover, in those existing studies, the longitudinal-axis control force was assumed to be available (general PN and ideal PN) or unavailable (true PN and pure PN). However, from the practical point of view, the longitudinal-axis control is generally not available during the terminal guidance process since the missile is not mounted with an extra thruster for this process. It is known that PN can provide better performance against the nonmaneuvering target or the low-maneuvering target. However, along with the development the modern weapon systems, the classical PN guidance laws and its generalization may not be adequate against the high-maneuvering target. As the maneuverability of the target increases, the performance of PN will become worse and lack of robustness (Zarchan [8]). To provide sufficient robustness of control law, Variable Structure Control (VSC) technique is applied in this paper to homing missile guidance design. The acceleration of the weaving target is treated as the external disturbance and the nonlinear characteristic of a missile-target interception process is also taken into account for the design.

It is known that VSC scheme possesses the advantages of fast response and less sensitivity to system uncertainties or disturbances than those by other methods. However, traditional VSC technique often results in a chattering behavior because of its discontinuous switching control law. The chattering behavior has some drawbacks including damage to mechanisms, excitation of unmodeled dynamics and waste of too much energy for reaching the sliding surface (see e.g., Slotine and Li [9]). Although the traditional boundary layer method with fixed boundary layer in VSC design can attenuate the degree of high-frequency behavior, its asymptotic stability performance cannot be guaranteed. Owing to these disadvantages of traditional variable structure control, in this paper, we employ VSC design technique to synthesize continuous control laws to reduce the control effort in both magnitude and frequency while ensuring asymptotically vanishing tracking error. Related research using VSC for an air-air interception problem can be found in Brierley and Longchamp [10] and Zhou et al. [11]. In those studies, they used fixed boundary layer to attenuate the chattering of high-frequency behavior. In this paper, we not only propose continuous VSC's to alleviate the chattering behavior by classic designs while guaranteeing asymptotically vanishing tracking error but also consider minimizing a quadratic performance index for reducing energy consumption of the control efforts in reduced-order dynamics with a prescribed degree of stability (Anderson and Moore [12]).

The organization of the paper is as follows. In Section 2, problem formulation is first given. It is followed by the design of continuous-type VSC control laws for the two cases of the longitudinal-axis control being available and unavailable. In Section 4, numerical simulations are presented and compared with those by Realistic True Proportional Navigation design (Yang and Yang [13]) to illustrate the use of the proposed scheme. Finally, Section 5 summarizes the main results.

2 Problem Formulation

This paper considers the design of guidance law for homing missile interception. The relative motion between a missile and its target is described by the spherical coordinate system with the origin fixed on the location of the missile as depicted in Fig. 1, where $\mathbf{e}_r$, $\mathbf{e}_\theta$, and $\mathbf{e}_\phi$ denote the three unit coordinate vectors in the spherical coordinate system, respectively.

For the design of the guidance law, we assume that both the missile and target are point masses and only system kinematics are considered. The governing equations for the relative motion is given by (Yang and Yang [13])

$$\ddot{r} - r\dot{\phi}^2 - r\dot{\theta}^2 \cos^2\phi = a_{Tr} - a_{Mr}, \tag{1}$$

$$r\dot{\theta}\cos\phi + 2\dot{r}\dot{\theta}\cos\phi - 2r\dot{\phi}\dot{\theta}\sin\phi = a_{T\theta} - a_{M\theta} \tag{2}$$

and

$$r\ddot{\phi} + 2\dot{r}\dot{\phi} + r\dot{\theta}^2\cos\phi\sin\phi = a_{T\phi} - a_{M\phi}. \tag{3}$$

Here, r is the relative distance between the missile and target, θ and ϕ are the azimuth and pitch angles, respectively, a_{Mr}, $a_{M\theta}$, and $a_{M\phi}$ denote the three commanded acceleration components of the missile in the spherical coordinates, which are to be designed to achieve the interception mission. In addition, a_{Tr}, $a_{T\theta}$, and $a_{T\phi}$ are the associated target's acceleration components in the spherical coordinates. Dynamical behavior of the system (1)–(3) has been studied (see e.g., Yang and Yang [13]; Meriam [14]). In this paper, the associated target's accelerations are assumed to be unpredictable and will be treated as disturbances in the design.

Contributed by the Dynamic Systems and Control Division for publication in the JOURNAL OF DYNAMIC SYSTEMS, MEASUREMENT, AND CONTROL. Manuscript received by the Dynamic Systems and Control Division February 4, 2000. Associate Technical Editors: E. Misawa and V. Utkin.

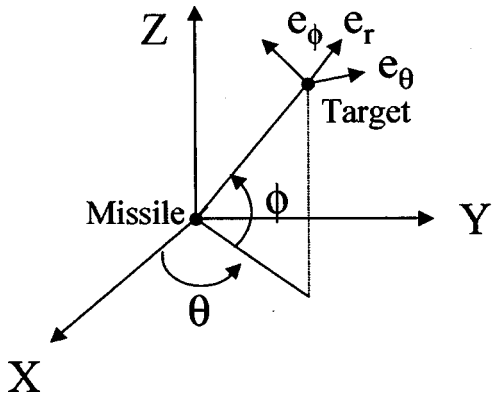

Fig. 1 Geometry of interception process

The goal of the paper then becomes to design a guidance law for achieving the interception mission. That is, to accomplish the performance of $r \to 0$.

3 Design of the Guidance Law

To achieve the main goal of the paper as stated in Section 2, in this section we employ the Variable Structure Control (VSC) technique to fulfill the design task. In general, VSC design procedure consists of three major steps (see e.g., DeCarlo [15]; Slotine and Li [9]). The first step is to choose a sliding surface, which is a function of system state. It is followed by the design of the controller for governing the motion on the sliding surface such that the reduced-order dynamics possesses desired stability performance. The final step is to construct an extra control for guaranteeing that the system state will reach the sliding surface in a finite time and forcing the system state to stay near the sliding surface. For the interception problem, we have the design as given below.

Let $\mathbf{x}=(\mathbf{x}_1^T,\mathbf{x}_2^T)^T$, where $\mathbf{x}_1=(x_1,x_2,x_3)^T=(r,\theta,\phi)^T$ and $\mathbf{x}_2=(x_4,x_5,x_6)^T=(\dot{r},\dot{\theta},\dot{\phi})^T$. The system equations (1)–(3) then become

$$\dot{\mathbf{x}}_1=\mathbf{x}_2 \tag{4}$$

and

$$\dot{\mathbf{x}}_2=\mathbf{f}(\mathbf{x})+G(\mathbf{x})(\mathbf{u}+\mathbf{d}), \tag{5}$$

where

$$\mathbf{f}(\mathbf{x})=\begin{pmatrix} f_1(\mathbf{x}) \\ f_2(\mathbf{x}) \\ f_3(\mathbf{x}) \end{pmatrix}=\begin{pmatrix} x_1x_6^2+x_1x_5^2\cos^2 x_3 \\ 2x_5x_6\tan x_3-\dfrac{2x_4x_5}{x_1} \\ -\dfrac{2x_4x_6}{x_1}-x_5^2\cos x_3\sin x_3 \end{pmatrix}, \tag{6}$$

$$G(\mathbf{x})=\begin{pmatrix} 1 & 0 & 0 \\ 0 & \dfrac{1}{x_1\cos x_3} & 0 \\ 0 & 0 & \dfrac{1}{x_1} \end{pmatrix}, \tag{7}$$

$$\mathbf{u}=(u_1,u_2,u_3)^T=(-a_{Mr},-a_{M\theta},-a_{M\phi})^T \tag{8}$$

and

$$\mathbf{d}=(d_1,d_2,d_3)^T=(a_{Tr},a_{T\theta},a_{T\phi})^T. \tag{9}$$

Note that, the dynamical system (4)–(5) is already in regular form (for definition, see e.g., DeCarlo et al. [15]).

In the following, we consider two cases for the design. One is to assume that the longitude-axis control force u_1 is available. The study of such a case without VSC design can be found, for instance, in Vathsal and Ros [16] and Yang and Yang [13]. The other case is that the applicable control forces contain u_2 and u_3 only since, in general, during the terminal guidance process, the missile is not mounted with a thruster in its longitude-axis.

3.1 Case for Longitude-Axis Control u_1 Being Available. First, we consider the case of longitude-axis control u_1 being available. Recall that the objective of the interception is to design a control law that makes the system state x_1 approaches zero (i.e., $r \to 0$). To fulfill this purpose and follow the VSC design procedure, we choose the sliding surface as

$$\mathbf{s}=(s_1,s_2,s_3)^T=\mathbf{x}_2+M\mathbf{x}_1=0, \tag{10}$$

where $M \in \mathbb{R}^{3\times 3}$ is a positive-definite matrix to be determined later. It is noted that, if the state lies on the sliding surface, the reduced model will have the form

$$\dot{\mathbf{x}}_1+M\mathbf{x}_1=0. \tag{11}$$

This implies that the performance $\mathbf{x}_1 \to 0$ exponentially, which achieves the main goal of the paper. In addition, the more positive-definiteness the matrix M as given in (10) is, the faster the speed of convergence the system state is. However, is might require more control energy. It is hence important to select a suitable matrix M to meet practical consideration. Suppose we now require that the motion on the sliding surface has a convergence speed close to $e^{-\alpha t}$ and the system motion on the sliding surface is optimal in the sense of minimizing the following cost function:

$$\int_0^\infty e^{2\alpha t}(\mathbf{x}_1^TQ\mathbf{x}_1+\mathbf{x}_2^T\mathbf{x}_2)dt, \tag{12}$$

where $Q=Q^T \geqslant 0$ is a constant matrix. Following the design procedure of Anderson and Moore [[12], pp. 60–62] by treating $\mathbf{x}_2$ as a virtual control input, the optimal control of Eq. (1) with cost function (12) is then obtained as $\mathbf{x}_2=-M\mathbf{x}_1$, where M satisfies the algebraic Riccati equation (ARE):

$$M(\alpha I)+(\alpha I)M-M^2+Q=0. \tag{13}$$

Here, I denotes the identity matrix.

The second step for VSC design is to synthesize the first part of control that governs system motion on the sliding surface, which will make the sliding surface an invariant manifold, i.e., $\dot{\mathbf{s}}=0$, in the absence of disturbances. From Eqs. (4)–(5) and (10), we have

$$\dot{\mathbf{s}}=M\mathbf{x}_2+\mathbf{f}(\mathbf{x})+G(\mathbf{x})(\mathbf{u}+\mathbf{d}). \tag{14}$$

Thus, the control force can then be obtained as

$$\mathbf{u}^{eq}=(u_1^{eq},u_2^{eq},u_3^{eq})^T=G^{-1}(\mathbf{x})[-\mathbf{f}(\mathbf{x})-M\mathbf{x}_2]. \tag{15}$$

The final step is to construct an extra control $\mathbf{u}^{re}=(u_1^{re},u_2^{re},u_3^{re})^T$ that can compensate for the effect of disturbances and guarantee the reaching condition. That is, to guarantee the system state reach the sliding surface in a finite time and stay near there hereafter even in the presence of disturbances. For this purpose, we impose the following assumption on the disturbance $\mathbf{d}$.

Assumption 3.1. There exist non-negative scalar functions $\rho_i(\mathbf{x})$ such that $|d_i| \leqslant \rho_i(\mathbf{x})$ for $i=1,2,3$.

To guarantee the reaching condition, we might select the controller from two classical VSC designs as given in (16)–(17) below (see e.g., Slotine and Li [9], DeCarlo et al. [15], Brierley and Longchamp [10]):

$$u_i^{re}=-(\rho_i(\mathbf{x})+\eta_i)\mathrm{sgn}(s_i) \quad \text{for} \quad i=1,2,3, \tag{16}$$

and

$$u_i^{re}=-(\rho_i(\mathbf{x})+\eta_i)\mathrm{sat}(s_i/\delta_i) \quad \text{for} \quad i=1,2,3. \tag{17}$$

In Eqs. (16)–(17), η_i and δ_i are positive constants, and sgn$(\cdot)$ and sat$(\cdot)$ denote the sign and saturation functions, respectively. The constants δ_i are referred to as the boundary layer widths of the sliding surfaces for saturation-type control. The overall control for VSC design is then constructed as $\mathbf{u}=\mathbf{u}^{eq}+\mathbf{u}^{re}$. Though these two types of controls might attain the desired performance, however, they inherit some drawbacks. First, the discontinuity of sign-type control as given in (16) leads to the chattering of system dynamics. In practical applications, chattering is generally undesirable since it involves extremely high control activity and might further excite high-frequency dynamics neglected in the course of modeling. Second, though the saturation-type controller as given in (17) is a continuous one, it has a constant width of boundary layer and the magnitude of $\mathbf{u}^{re}$, as given in (16), reduces to zero as the system state approaches the sliding surface. This might result in the magnitude of control effort smaller than those of disturbances when system states lie within the boundary layer. Thus, the saturation-type control can only guarantee the system state entering the boundary layer but not providing the asymptotic stability in the presence of disturbances.

In the following, instead of using the control designs as in (16)–(17), a continuous control law is proposed below to alleviate the chattering behavior while retaining the system performance of exponential stability. The proposed control is modified from the saturation-type controller. To this end, we define the following functions

$$g_i(s_i)=\frac{2s_i}{|s_i|+\epsilon_i e^{-\gamma_i t}},\quad i=1,2,3 \tag{18}$$

with $\epsilon_i>0$ and $\gamma_i>0$, which will be selected by the designer. The overall control law $\mathbf{u}=(u_1,u_2,u_3)^T$ for guidance can then be modified as

$$u_i=u_i^{eq}-(\rho_i(\mathbf{x})+\eta_i)g_i(s_i)\ \text{ for }\ i=1,2,3 \tag{19}$$

with u_i^{eq} as given in (15). Note that, the modified control law in (19) above is defined and continuous everywhere including the sliding surface.

The idea behind the modified guidance law is to construct a time-varying region $\Phi_\beta(\mathbf{x},t)$ of the sliding surface as defined by

$$\Phi_\beta(\mathbf{x},t)=\{\mathbf{x}\,|\,|s_i(\mathbf{x})|\leqslant\beta\cdot\epsilon_i e^{-\gamma_i t}\ \text{ for }\ i=1,2,3\ \text{ with }\ \beta\geqslant 1\}. \tag{20}$$

By defining the width of the region $\Phi_\beta(\mathbf{x},t)$ to be $\min_{i=1,2,3}\{\beta\epsilon_i e^{-\gamma_i t}\}$, it is clear that the width of $\Phi_\beta(\mathbf{x},t)$ exponentially converges to zero.

Now, we will show that, under the modified guidance law (19), the performance of the design can be achieved. First, consider the case when the system state is outside the region $\Phi_1(\mathbf{x},t)$ $(=\Phi_\beta(\mathbf{x},t)|_{\beta=1})$. That is, $|s_i(\mathbf{x})|\geqslant 1\cdot\epsilon_i e^{-\gamma_i t}$ for some $i=1,2,3$. During the interception process, it is reasonable to assume that $x_1>0$, $|\phi|<\pi/2$ and the relative distance r between the target and missile is smaller than the initial relative distance r_0. This implies that $G_{ii}(\mathbf{x})>0$ for all $i=1,2,3$ and $|G_{ii}(\mathbf{x})|\geqslant 1/r_0$ for $i=1,2$, where $G_{ii}(\mathbf{x})$ denotes the (i,i)-entry of the matrix $G(\mathbf{x})$. From Eqs. (7), (14), (19), and Assumption 3.1, we have

$$\begin{aligned} s_i\dot{s}_i &= s_i\cdot[G_{ii}(\mathbf{x})(u_i^{re}+d_i)] \\ &\leqslant -G_{ii}(\mathbf{x})(\rho_i(\mathbf{x})+\eta_i)\cdot\frac{2s_i^2}{2|s_i|}+G_{ii}(\mathbf{x})\rho_i(\mathbf{x})\cdot|s_i| \\ &\leqslant -\eta_i G_{ii}(\mathbf{x})\cdot|s_i|. \end{aligned} \tag{21}$$

Thus, the system state will reach the time-varying region $\Phi_1(\mathbf{x},t)$ in a finite time. In fact, the reaching time t_{reach} can be calculated and satisfies the relationship: $t_{\text{reach}}\leqslant\max_{1\leqslant i\leqslant 3}\{|s_i(\mathbf{x}_0)|\cdot r_0/\eta_i\}$, where $\mathbf{x}_0$ denotes the initial state and the initial time is assumed to be $t=0$. Moreover, for any given $\beta>1$, it is noted from (21) that $1/2(d/dt)s_i^2=\dot{s}_i s_i<0$ for all the system state within the set $\Phi_\beta(\mathbf{x},t)\backslash\Phi_1(\mathbf{x},t)$. It implies that, for $\beta>1$, the time-varying region $\Phi_\beta(\mathbf{x},t)$ is an attractive and invariant set for the closed-loop dynamics. That is, the system state will reach the region $\Phi_\beta(\mathbf{x},t)$ and it will stay inside there hereafter once it enters this region. We then have the next result.

Theorem 3.1. Suppose the disturbances $\mathbf{d}$ satisfy Assumption 3.1. Then the interception performance for system (4)–(5) can be achieved at an exponential rate by the VSC control law as in (19) if $\gamma_i>\lambda_{\max}(M)-\lambda_{\min}(M)$ for all $i=1,2,3$, where $\lambda_{\min}(\cdot)$ and $\lambda_{\max}(\cdot)$, respectively, denote the smallest and largest eigenvalues and M satisfies Eq. (13).

Proof: From the discussions above for $\beta>1$, we know that the system state will enter the region $\Phi_\beta(\mathbf{x},t)$ in a finite time and remain inside there hereafter. It remains to show that $\mathbf{x}_1\to 0$ as $t\to\infty$ for any $\mathbf{x}\in\Phi_\beta(\mathbf{x},t)$. By the definition of $\mathbf{s}(\mathbf{x})=\dot{\mathbf{x}}_1+M\mathbf{x}_1$, we then have

$$\mathbf{x}_1(t)=e^{-Mt}\mathbf{x}_1(0)+\int_0^t e^{-M(t-\tau)}\mathbf{s}(\mathbf{x}(\tau))d\tau. \tag{22}$$

Since $M>0$, this implies that $e^{-Mt}\mathbf{x}_1(0)\to 0$ exponentially as $t\to\infty$. Moreover, since $x\in\Phi_\beta(\mathbf{x},t)$, we have $\|\mathbf{s}(\mathbf{x})\|\leqslant\Sigma_{i=1}^3|\beta\epsilon_i e^{-\gamma_i t}|$, where $\|\cdot\|$ denotes the Euclidean norm and

$$\begin{aligned} &\left\|\int_0^t e^{-M(t-\tau)}\mathbf{s}(\mathbf{x}(\tau))d\tau\right\| \\ &\leqslant\|e^{-Mt}\|\cdot\int_0^t\|e^{M\tau}\|\cdot\|\mathbf{s}(\mathbf{x}(\tau))\|d\tau \\ &\leqslant\sum_{i=1}^3\beta\epsilon_i\left(e^{-\lambda_{\min}(M)t}\cdot\int_0^t e^{\lambda_{\max}(M)\tau}\cdot e^{-\gamma_i\tau}d\tau\right) \\ &\leqslant\sum_{i=1}^3\beta\epsilon_i h_i(t) \end{aligned} \tag{23}$$

with

$$h_i(t)=\begin{cases} te^{-\lambda_{\min}(M)t} & \text{if }\ \gamma_i=\lambda_{\max}(M), \\ e^{-\lambda_{\min}(M)t}\left[\dfrac{1}{\lambda_{\max}(M)-\gamma_i}(e^{(\lambda_{\max}(M)-\gamma_i)t}-1)\right] & \text{if }\ \gamma_i\neq\lambda_{\max}(M). \end{cases} \tag{24}$$

By L'Hospital rule (see e.g., Buck [17]), if $\gamma_i>\lambda_{\max}(M)-\lambda_{\min}(M)$, then $h_i(t)\to 0$ as $t\to\infty$. From (22)–(23), we have $\mathbf{x}_1\to 0$ exponentially as $t\to\infty$ if $\gamma_i>\lambda_{\max}(M)-\lambda_{\min}(M)$ for all $i=1,2,3$. This completes the proof. ■

Remark 3.1. The control law as provided in Theorem 3.1 is continuous and alleviates the chattering behavior, which improves the drawbacks inherited from those derived from sign function.

3.2 Case for Longitude-Axis Control u_1 Being Unavailable. Next, we consider the case of u_1 being unavailable. That is, the control $\mathbf{u}$ in (19) is reduced as $\mathbf{u}=(0,u_2,u_3)^T$. It is observed from Eq. (6) that $\mathbf{f}(\mathbf{x})$ becomes a null vector when $x_1\neq 0$ and $x_5=x_6=0$. Then, from (4)–(5), $x_5(t)\cong 0$, $x_6(t)\cong 0$ for all $t\geqslant t_0$ and $x_4(t)$ approaches a finite value if $x_5(t_0)=0$, $x_6(t_0)=0$ and the disturbances $\mathbf{d}$ is suitably compensated by the control $\mathbf{u}$. As mo-

tivated by such observation, we can choose $x_5=0$ and $x_6=0$ as new sliding surface for VSC guidance design. Instead of constructing a tracking control law as proposed in Section 3.1 to steer x_i to zero for all $i=1,\ldots,6$, in the following, we only need to check whether x_1 approaches zero without the control u_1 while x_5 and x_6 reaching the sliding surface: $x_5=0$ and $x_6=0$. Details are given below.

Choose the sliding surface $\mathbf{s}=(s_1,s_2)^T=(x_5,x_6)^T=(0,0)^T$. Following the same procedure as discussed in Section 3.1, the guidance law can then be selected as

$$u_i=u_i^{eq}+u_i^{re} \text{ for } i=2,3, \tag{25}$$

where

$$u_i^{eq}=-G_{ii}^{-1}(\mathbf{x})f_i(\mathbf{x}) \tag{26}$$

and

$$u_i^{re}=-(\rho_i(\mathbf{x})+\eta_i)g_i(s_{i-1}). \tag{27}$$

Here, $\rho_i(\mathbf{x})$, η_i and $g_i(\cdot)$ are as defined in Section 3.1. Similarly, under the above guidance law, we have

$$s_{i-1}\dot{s}_{i-1}\leqslant-\eta_i G_{ii}(\mathbf{x})\cdot|s_{i-1}| \text{ for } i=2,3. \tag{28}$$

Thus, the system states will reach the sliding surface in a finite time and the reaching time $t_{\text{reach}}\leqslant\max\{|s_2(\mathbf{x}_0)|\cdot r_0/\eta_2, |s3(\mathbf{x}0)|\cdot r0/\eta3\}$.In addition, similar to the discussions in Section 3.1, we can show that the set $\Phi_\beta(\mathbf{x},t)=\{\mathbf{x}||s_i(\mathbf{x})|\leqslant\beta\cdot\epsilon_i e^{-\gamma_i t}, i=2,3\}$ is attractive and invariant for the closed-loop dynamics for any $\beta>1$.

Now, we will check the condition to guarantee $x_1\to0$ during the interception with $u_1=0$. Denote t_f the time of interception such that $x_1(t_f)=0$. From (5) and Assumption 3.1, we have

$$\begin{aligned}x_4(t)-x_4(0)&\leqslant\int_0^t\{x_1[x_5^2\cos^2x_3+x_6^2]+\rho_1(\mathbf{x})\}d\tau\\&\leqslant\int_0^{t_f}\{x_1[x_5^2\cos^2x_3+x_6^2]+\rho_1(\mathbf{x})\}d\tau\end{aligned} \tag{29}$$

for all $0\leqslant t\leqslant t_f$. To guarantee the interception, we require that

$$x_4(t)\leqslant-k \text{ for some } k>0 \tag{30}$$

during the interception process. From (29), this can be achieved if

$$x_4(0)\leqslant-k-\int_0^{t_f}\{x_1[x_5^2\cos^2x_3+x_6^2]+\rho_1(\mathbf{x})\}dt. \tag{31}$$

We then have the next result.

Theorem 3.2. Suppose the disturbances **d** satisfy Assumption 3.1 and the longitudinal-axis control is unavailable (i.e., $u_1=0$). Then, the interception performance for system (4)–(5) can be achieved by the control laws as given in (25) if there exists a $k>0$ such that condition (31) holds.

To further estimate the initial relative velocity $x_4(0)$ for guaranteeing the success of interception, suppose that the relative velocity satisfies (30). Then by integrating the first equation of (4) with $x_1(t_f)=0$, we have

$$-x_1(0)=\int_0^{t_f}x_4(t)dt\leqslant\int_0^{t_f}-kdt\leqslant-kt_f. \tag{32}$$

This implies that

$$t_f\leqslant r_0/k. \tag{33}$$

Since $x_1(0)=r_0$ and $\dot{x}_1(t)\leqslant-k$ for all t during the interception process, we have

$$x_1(t)\leqslant r_0-kt \text{ for } 0\leqslant t\leqslant t_f. \tag{34}$$

Denote t_5 and t_6 the first time that the state x_5 and x_6 enter the region $\Phi_1(\mathbf{x},t)$. It follows from (33)–(34) that

$$\begin{aligned}&\int_0^{t_f}x_1x_5^2\cos^2x_3dt\\&\leqslant\int_0^{t_5}x_1x_5^2dt+\int_{t_5}^{t_f}x_1x_5^2dt\\&\leqslant\int_0^{t_5}(r_0-kt)x_5^2(0)dt+\int_{t_5}^{r_0/k}(r_0-kt)(\epsilon_2e^{-\gamma_2t})^2dt\\&=x_5^2(0)\left[r_0t_5-\frac{kt_5^2}{2}\right]+\left(\frac{r_0\epsilon_2^2}{2\gamma_2}+\frac{k\epsilon_2^2}{4\gamma_2^2}-t_5\frac{k\epsilon_2^2}{2\gamma_2}\right)e^{-2\gamma_2t_5}\\&\quad-\frac{k\epsilon_2^2}{4\gamma_2^2}e^{-2\gamma_2r_0/k}.\end{aligned} \tag{35}$$

Here, we have used the fact that, after x_5 enter the region $\Phi_1(\mathbf{x},t)$, $|x_5|\leqslant\epsilon_2e^{-\gamma_2t}$. Similarly, it can be shown that

$$\begin{aligned}\int_0^{t_f}x_1x_6^2dt\leqslant x_6^2(0)&\left[r_0t_6-\frac{kt_6^2}{2}\right]+\left(\frac{r_0\epsilon_3^2}{2\gamma_3}+\frac{k\epsilon_3^2}{4\gamma_3^2}-t_6\frac{k\epsilon_3^2}{2\gamma_3}\right)e^{-2\gamma_3t_6}\\&-\frac{k\epsilon_3^2}{4\gamma_3^2}e^{-2\gamma_3r_0/k}.\end{aligned} \tag{36}$$

Combining (35), (36), and (31), we thus have the next result which is independent of t_f.

Corollary 3.1. Suppose the disturbances **d** satisfy Assumption 3.1 and the longitudinal-axis control is unavailable (i.e., $u_1=0$). Then, the interception performance for system (4)–(5) can be achieved by the control laws as given in (25) if there exists a $k>0$ such that the initial relative velocity satisfies the following condition:

$$\begin{aligned}x_4(0)\leqslant-k-\sum_{j=2}^{3}&\left\{x_{j+3}^2(0)\left[r_0t_{j+3}-\frac{kt_{j+3}^2}{2}\right]+\left(\frac{r_0\epsilon_j^2}{2\gamma_j}+\frac{k\epsilon_j^2}{4\gamma_j^2}\right.\right.\\&\left.\left.-t_{j+3}\frac{k\epsilon_j^2}{2\gamma_j}\right)e^{-2\gamma_jt_{j+3}}-\frac{k\epsilon_j^2}{4\gamma_j^2}e^{-2\gamma_jr_0/k}\right\}-\int_0^{r_0/k}\rho_1(\mathbf{x})dt.\end{aligned} \tag{37}$$

For the case of $t_5=t_6=0$, that is, the initial state lies within the region $\Phi_1(\mathbf{x},t)$, we have the next result.

Corollary 3.2. Suppose that $|x_5(0)|\leqslant\epsilon_2$ and $|x_6(0)|\leqslant\epsilon_3$. Then, the results of Theorem 3.2 hold if there exists a $k>0$ such that the initial relative velocity satisfies the following condition:

$$x_4(0)\leqslant-k-\sum_{j=2}^{3}\left\{\frac{r_0\epsilon_j^2}{2\gamma_j}+\frac{k\epsilon_j^2}{4\gamma_j^2}(1-e^{-2\gamma_jr_0/k})\right\}-\int_0^{r_0/k}\rho_1(\mathbf{x})dt. \tag{38}$$

Note that, if $d_1=0$, then $\rho_1(\mathbf{x})$ may be chosen as the zero function. The condition as in (38) might be simplified. Denote

$$F(k)=-k-\sum_{j=2}^{3}\left\{\frac{r_0\epsilon_j^2}{2\gamma_j}+\frac{k\epsilon_j^2}{4\gamma_j^2}(1-e^{-2\gamma_jr_0/k})\right\}. \tag{39}$$

By calculation, we have the derivative

$$\frac{dF(k)}{dk}=1-\sum_{j=2}^{3}\left\{\frac{\epsilon_j^2}{4\gamma_j^2}\left(1-e^{-2r_0\gamma_j/k}-\frac{2r_0\gamma_j}{k}e^{-2r_0\gamma_j/k}\right)\right\}. \tag{40}$$

This implies that $dF(k)/dk<0$ if

$$\sum_{j=2}^{3}\left\{\frac{\epsilon_j^2}{4\gamma_j^2}\left(1+\frac{2r_0\gamma_j}{k}\right)e^{-2r_0\gamma_j/k}\right\}<1+\sum_{j=2}^{3}\frac{\epsilon_j^2}{4\gamma_j^2}. \tag{41}$$

By L'Hospital rule, we have $(1+2r_0\gamma_j/k)e^{-2r_0\gamma_j/k}\to0$ as $k\to0$. It follows that condition (41) holds in a neighborhood of k

$=0$. That is, $F(k)$ is a decreasing function of k in a neighborhood of $k=0$. Define $F(0)=\lim_{k\to 0}F(k)$. It is clear that $F(k)$ is a continuous function. Thus, if $x_4(0)<F(0)=-\Sigma_{j=2}^{3}r_0\epsilon_j^2/2\gamma_j$, then there exists a $k>0$ such that $x_4(0)<F(k)$. The next result follows readily from Corollary 3.2.

Corollary 3.3. Suppose that $|x_5(0)|\leq\epsilon_2$, $|x_6(0)|\leq\epsilon_3$ and $d_1=0$. Then, the results of Theorem 3.2 hold if $x_4(0)$ satisfies the following estimation:

$$x_4(0)<-\sum_{j=2}^{3}\frac{r_0\epsilon_j^2}{2\gamma_j}. \tag{42}$$

4 Simulation Results

In this section, we present an example to demonstrate the use of the main results. The target in this example is considered for both maneuvering and nonmaneuvering cases. For the maneuvering case, the target's acceleration is assumed to be in the direction orthogonal to the line of sight (LOS) and has the form

$$\mathbf{a}_T=\sin(0.1t)\mathbf{e}_\theta+\cos(0.1t)\mathbf{e}_\phi. \tag{43}$$

In 1996, Yang and Yang proposed a realistic true proportional navigation (RTPN) guidance law, which has the form

$$\mathbf{a}_M=-\lambda\dot{r}(\dot{\theta}\cos\phi\mathbf{e}_\theta+\dot{\phi}\mathbf{e}_\phi). \tag{44}$$

It was shown (Yang and Yang [13]) that the target can be successfully intercepted if the following condition is satisfied:

$$\frac{|\dot{r}_0|}{h_0/r_0}>\frac{1}{\sqrt{\lambda-1}}, \tag{45}$$

where $h_0=r_0^2\sqrt{\dot{\phi}_0^2+\dot{\theta}_0^2\cos^2\phi_0}$. To fulfill the requirement of (45), in this example, $\lambda=3$ and the initial state is chosen as $r_0=5$ km, $\theta_0=-0.2$ rad, $\phi_0=0.1$ rad, $\dot{r}_0=-0.51$ km/hr, $\dot{\theta}_0=-0.01$ rad/hr and $\dot{\phi}_0=0.05$ rad/hr.

In addition to the initial condition in the proposed design, the convergence rate α and the matrix Q in (12) are, respectively, selected as $\alpha=1$ and the identity matrix. The solution matrix M of the algebraic Riccati equation (13) is then calculated to be

$$M=\text{diag}\{2.414, 2.414, 2.414\}. \tag{46}$$

Moreover, the parameters are chosen to be $\epsilon_1=0.2$, $\epsilon_2=\epsilon_3=0.1$, $\gamma_1=\gamma_2=\gamma_3=0.1$, $\eta_1=1$, $\eta_2=\eta_3=0.1$, and the three nonnegative functions in Assumption 3.1 have the form $\rho_1(\mathbf{x})=0$, $\rho_2(\mathbf{x})=1$ and $\rho_3(\mathbf{x})=1$. Note that, under the selection of parameters, the criterion (42) in Corollary 3.3 is satisfied. This means that the interception performance can be achieved by the proposed VSC designs as given in Section 3.

Numerical simulations are given in Figs. 2–5. Among these, Fig. 2 displays the time responses of the system states for the nonmaneuvering case by VSC and RTPN designs. The associated control efforts are depicted in Fig. 3 and the relative trajectories during interception are given in Fig. 4. Figure 5 shows the time responses of the system states for maneuvering case with target's acceleration being given by (43). In these figures, dotted line (labeled by VSC1), dash-dotted line (labeled by VSC0) and solid line (labeled by RTPN) denote the response curves resulted from the use of VSC control with u_1 being available, VSC control with u_1 being unavailable and RTPN control, respectively. It is observed from Fig. 2 that the interception performance can be achieved for the nonmaneuvering case by all of the three control designs. The VSC1 curve exhibits exponential convergence rate, which agrees with the results of the paper, while VSC0 and RTPN display linear decay. Moreover, as observed from Fig. 2, all the

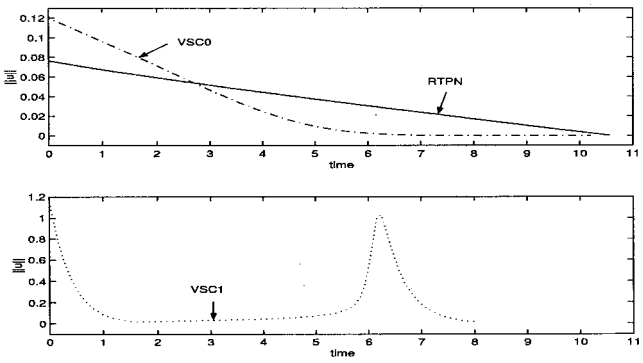

Fig. 3 Norm of controls for nonmaneuvering case with VSC and RTPN case

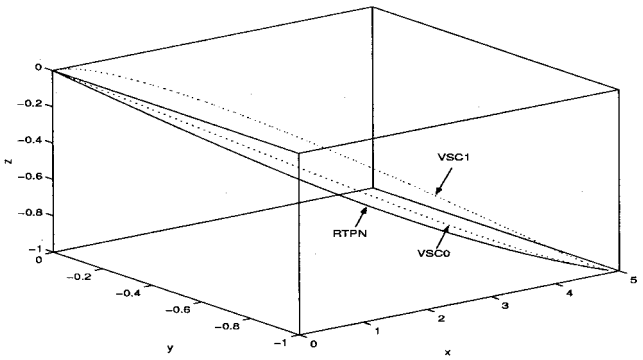

Fig. 4 Relative interception trajectories for nonmaneuvering target case with VSC and RTPN controls

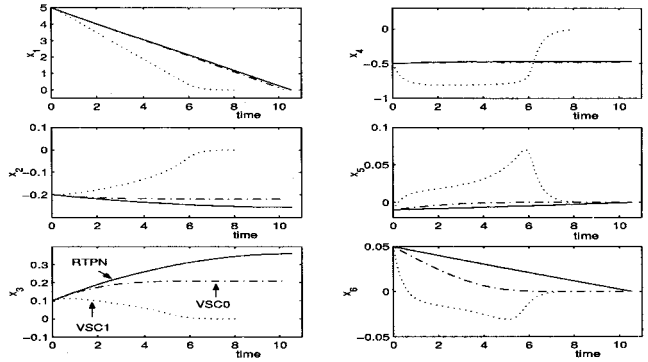

Fig. 2 Responses for nonmaneuver target case with VSC and RTPN controls

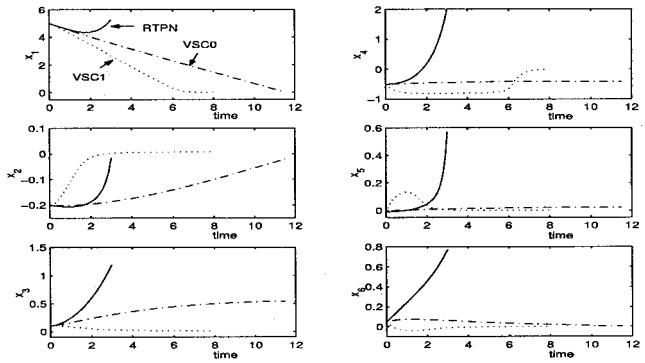

Fig. 5 Responses for maneuvering target case with VSC and RTPN controls

six states approach zero by VSC1 design, while $x_i \to 0$ for $i = 3, \cdots, 6$ by VSC0 design. These agree with the designs proposed in Section 3. Although the interception time of VSC1 curve is shorter than those by VSC0 and RTPN designs, however, as depicted in Fig. 3, more energy consumption is required. The second peak of the curve VSC1 at around $t = 6.2$ in Fig. 3 results from bringing the states x_4, x_5, and x_6 to zero value. It is observed from Fig. 3 that the scale of the interception time and energy consumption is very close by both RTPN and VSC0 designs. However, for maneuvering case as depicted in Fig. 5, the target is intercepted by two VSC guidance laws but not by the RTPN design. From this example, it can be concluded that the proposed VSC guidance law is more robust than that of RTPN guidance law, especially, for maneuvering case.

5 Conclusions

VSC type of guidance laws have been proposed in this paper to study terminal guidance problem for the cases of longitudinal-axis control being available and unavailable. By the use of VSC technique and the optimal control strategy with respect to the motion on sliding surface, the proposed guidance laws have been shown to be able to achieve the interception performance and alleviate the chattering drawback. An illustrative example was also given to demonstrate the use of the main results and compare system performances with those by RTPN design. It is shown that VSC design is more robust than the RTPN scheme, especially, for maneuvering case.

Acknowledgments

The authors are grateful to the reviewers for their comments and suggestions. This research was supported by the National Science Council, Taiwan, R.O.C. under Grants NSC 84-2212-E009-002 and NSC 89-CS-D-009-013.

References

[1] Axelband, E. Z., and Hardy, F. W., 1970, ''Quasi Optimal Proportional Navigation,'' IEEE Trans. Autom. Control, **AC-15**, No. 6, pp. 620–626.
[2] Arbenz, K., 1970, ''Proportional Navigation of Nonstationary Targets,'' IEEE Trans. Aerosp. Electron. Syst., **AES-6**, No. 4, pp. 455–457.
[3] Kim, Y. S., Cho, H. S., and Bien, Z., 1985, ''A New Guidance Law for Homing Missile,'' J. Guid. Control Dyn., **8**, No. 3, pp. 402–404.
[4] Yang, C.-D., and Yeh, F. B., 1989, ''General Guidance Law for Homing Missile,'' IEEE Trans. Aerosp. Electron. Syst., **25**, No. 2, pp. 197–211.
[5] Becker, K., 1990, ''Closed-form Solution of Pure Proportional Navigation,'' IEEE Trans. Aerosp. Electron. Syst., **26**, No. 3, pp. 526–532.
[6] Yuan, P. J., and Chern, J. S., 1992, ''Ideal Proportional Navigation,'' J. Guid. Control Dyn., **15**, No. 5, pp. 1161–1165.
[7] Yuan, P. J., and Chern, J. S., 1992, ''Solutions of True Proportional Navigation for Maneuvering and Nonmaneuvering Targets,'' J. Guid. Control Dyn., **15**, No. 1, pp. 268–271.
[8] Zarchan, P., 1995, ''Proportional Navigation and Weaving Targets,'' J. Guid. Control Dyn., **18**, No. 5, pp. 969–974.
[9] Slotine, J.-J. E. and Li, W., 1991, *Applied Nonlinear Control*, Prentice-Hall, New Jersey.
[10] Brierley, S. D., and Longchamp, R., 1990, ''Application of Sliding-Mode Control to Air-Air Interception Problem,'' IEEE Trans. Aerosp. Electron. Syst., **26**, No. 2, pp. 306–324.
[11] Zhou, D., Chundi, M., and Wenli, X., 1999, ''Adaptive Sliding-Mode Guidance of a Homing Missile,'' J. Guid. Control Dyn., **22**, No. 4, pp. 589–594.
[12] Anderson, B. D. O., and Moore, J. B., 1990, *Optimal Control: Linear Quadratic Methods*, Prentice-Hall, New Jersey.
[13] Yang, C.-D., and Yang, C.-C., 1996, ''Analytical Solution of Three-Dimensional Realistic True Proportional Navigation,'' J. Guid. Control Dyn., **19**, No. 3, pp. 569–577.
[14] Meriam, J. L., 1975, *Dynamics*, 2nd Ed., SI version, Wiley, New York.
[15] DeCarlo, R. A., Zak, S. H., and Matthews, G. P., 1988, ''Variable Structure Control of Nonlinear Multivariable Systems: A Tutorial,'' Proc. IEEE, **76**, pp. 212–232.
[16] Vathsal, S., and Rao, M. N., 1995, ''Analysis of Generalized Guidance Laws for Homing Missile,'' IEEE Trans. Aerosp. Electron. Syst., **31**, No. 2, pp. 514–521.
[17] Buck, R. C., 1978, *Advanced Calculus*, 3rd Ed., McGraw-Hill, New York.